

More on String Breaking in the 3D Abelian Higgs Model: the Photon Propagator

M. N. Chernodub^{a,b}, E.–M. Ilgenfritz^c and A. Schiller^d

^a *ITEP, B. Chermushkinskaya 25, Moscow, 117259, Russia*

^b *Institute for Theoretical Physics, Kanazawa University,
Kanazawa 920-1192, Japan*

^c *Institut für Physik, Humboldt–Universität zu Berlin, D-10115 Berlin, Germany*

^d *Institut für Theoretische Physik and NTZ, Universität Leipzig,
D-04109 Leipzig, Germany*

Abstract

We study the Landau gauge photon propagator in the three–dimensional Abelian Higgs model with compact gauge field and fundamentally charged matter in the London limit. The total gauge field is split into singular and regular parts. On the confinement side of the string breaking crossover the momentum dependence of the total propagator is characterized by an anomalous dimension similarly to 3D compact QED. At the crossover and throughout the Higgs region the anomalous dimension disappears. This result perfectly agrees with recent observations that the monopole–antimonopole plasma leads to nonzero anomalous dimension and the presence of the matter fields causes monopole pairing into dipole bound states. The Yukawa mass characterizing the propagator part from regular gauge fields is non-vanishing at the Higgs side and coincides with the mass found for the total propagator. The regular gauge field without anomalous dimension becomes massless at the crossover and in the confinement region.

1 Introduction

Nowadays, the interest in the lattice Abelian Higgs model with compact gauge field (cAHM) in three dimensions has grown because of its relation to high energy physics [1, 2] and its applications in condensed matter physics [3].

The compactness of the gauge field leads to the presence of monopoles which are instanton-like excitations in three space-time dimensions. Being in the plasma state the monopoles and antimonopoles of this theory guarantee linear confinement of electrically charged test particles [4]. They are forming an oppositely charged double sheet along the minimal surface spanned by the Wilson loop (i.e. the trajectories of the heavy charges). Due to screening, the free energy of the surface increases proportionally to the area of the surface such that an area law for the Wilson loop emerges.

Within the confinement region of cAHM corresponding to small couplings of matter fields to gauge fields the monopole-antimonopole plasma state is still realized. As the hopping parameter increases, the system enters the Higgs region where monopoles and antimonopoles become bound into magnetically neutral dipoles. This scenario has been demonstrated in a preceding paper [5] and it has been related to the phenomenon of string breaking. Indeed, when monopole pair formation occurs, this results in the breakdown of linear confinement at large distances. Usually this is interpreted in an alternative way saying that dynamical matter fields in the same representation as the external test charges break the confining string by screening the charge of the latter. This argument is applied, irrespective whether the dynamical matter field is fermionic (the quarks in QCD) or bosonic (the Higgs particles in our case). Let us stress here the other point of view, according to which the monopole mechanism of confinement is changed in a way to produce a different form of the inter-particle potential. At large separations R of the charges the string tension should be absent. However, if $R \ll R_{\text{br}}$ (where R_{br} is the characteristic string breaking distance) the test charges are able to recognize individual monopoles even if they are bound in dipoles. Therefore, the monopole and antimonopole fields may induce a piecewise linearly rising potential. These simple considerations can be made more rigorous by analytical calculations [6] for a gas of dipoles with small magnetic moments.

In order to destroy the linearly rising potential within cAHM₃, the coupling between Higgs and gauge fields must be sufficiently strong. It would be tempting to associate the onset of string breaking with a phase transition between confinement and Higgs phases. However, it was numerically shown [5] that in the London limit of cAHM₃ the string breaking happens in a region of the phase diagram where a first or second order phase transition can definitely be excluded. In the present paper we will call this the “string breaking crossover”, but one should keep in mind that a thorough reconstruction of the monopole configurations is accompanying this. However, the possibility [3] that string breaking (and monopole pairing) is associated with a Berezinsky-Kosterlitz-Thouless (BKT) type transition [7] is not ruled out.

Recently, it was found that the matter fields in the Abelian Higgs model lead to a logarithmic attraction between monopoles and antimonopoles [3] which would explain the formation of monopole-antimonopole bound states and string breaking. Adding massless quarks also forces the Abelian monopoles and antimonopoles to form bound states [8]. Note that the origin of monopole binding in the zero temperature case of the cAHM₃ is physically different from the monopole binding observed at the finite temperature phase transition in compact (2 + 1)-dimensional pure QED [9, 10].

We have recently studied the effect of finite temperature deconfinement of (2+1)-dimensional cQED on the photon propagator in Refs. [11, 12]. We could demonstrate that the momentum behaviour of the photon propagator in this theory is described, rather similar to gluodynamics, by a Debye mass and by an anomalous dimension which both vanish at the deconfinement transition. This mechanism could be clearly attributed to pairing of magnetic monopoles. The monopole-antimonopole plasma contribution is relatively easy to exhibit by explicit calculation and can be eliminated by *monopole subtraction* from the ensemble of gauge fields.

As for gluodynamics, which motivated our study of the cAHM₃, numerical lattice results show that the propagator for all these gauges in momentum space is less singular than $1/p^2$ in the immediate vicinity of $p^2 = 0$. Recent investigations in the Landau gauge and in the Laplacian gauge¹ show that, beside the suppression at $p^2 \rightarrow 0$, the propagator is enhanced at intermediate momenta which can be characterized by an anomalous dimension [15]. This enhancement of the Landau gauge propagator in $SU(2)$ gluodynamics has been interpreted [16] by focusing on P -vortices appearing in the maximal center gauge. Subtracting the vortices removes the enhancement at intermediate momenta. The results for the propagator at zero momentum are ranging from a finite [14] (Laplacian gauge) to a strictly vanishing [13, 17, 18] (Coulomb gauge) value. The vanishing of the Landau gauge propagator at $p^2 = 0$, suggested by considering the Faddeev-Popov mechanism, remains obscured so far in the results, probably because the lattices are still too small.

In this paper we are going to investigate in which way the photon propagator within cAHM₃ changes at the string breaking crossover, turning from confinement to the symmetry-broken Higgs region. As in our previous work we have chosen the propagator in the minimal Landau gauge because this is the covariant gauge which has been adopted in most of the investigations of the gauge boson propagators in QCD [15, 16] and QED [19]. For the behaviour at the string breaking crossover of cAHM₃ we anticipate that a confining propagator will change into a Yukawa-like propagator corresponding to the onset of the Higgs mechanism.

The present paper is structured as follows. Next, in Section 2, we will recall the model and the definition of the photon propagator. The form of the fitting function and the method of monopole subtraction are also introduced there. In Section 3 we will report the numerical results of the present study and discuss the sensitivity with respect to the Gribov copy problem. We conclude in Section 4.

2 The Model and the Definition of the Propagator

We consider the three-dimensional Abelian gauge model with compact gauge fields $\theta_{x,\mu}$ living on links and a fundamentally charged Higgs fields Φ_x on sites. For simplicity we consider the London limit of the model, which corresponds to an infinitely deep potential for the Higgs field. Consequently, the radial part of the Higgs field, $|\Phi_x|$, gets frozen. With $\varphi_x = \arg \Phi_x$ we define the model by the action

$$S[\theta] = -\beta \sum_P \cos \theta_P - \kappa \sum_{x,\mu} \cos(\theta_{x,\mu} + \varphi_{x+\hat{\mu}} - \varphi_x), \quad (1)$$

¹In order to avoid the problem of Gribov copies [13], the alternative Laplacian gauge has also been used recently [14] in Yang-Mills theory. However, principal questions of renormalizability and transversality are yet unsolved in this case.

where β is the inverse gauge coupling squared, κ is the hopping parameter, and θ_P is the plaquette angle representing the curl of the link field $\theta_{x,\mu}$.

For the simulations we use a Monte Carlo algorithm similar to the one described in Refs. [11, 12, 5]. The Higgs field angles have been updated in alternating order with the gauge field angles. In both cases, one 5-hit Metropolis sweep together with 2 microcanonical sweeps constitute a total gauge or Higgs update. Global updates of the gauge field have a negligible acceptance rate for $\kappa \neq 0$. They have been discarded at all. The numerical calculations have been carried out for fixed gauge coupling, $\beta = 2.0$, on lattices of size 32^3 , as in Ref. [5]. For these parameters, the low- κ region (“confinement region”) and the high- κ region (“Higgs region”) of the phase diagram are separated by a crossover. The crossover point — observed as a position of the peak of the susceptibility of the hopping term $S_{GH} = \sum_{x,\mu} \cos(\theta_{x,\mu} + \varphi_{x+\hat{\mu}} - \varphi_x)$ — is located at $\kappa_c = 0.526(1)$. We have considered from $O(200)$ to $O(400)$ independent configurations (obtained after 10 subsequent updates) to measure the propagator.

The discussion of the photon propagator (and its various parts) is given in lattice momentum space. Being always defined in the context of a specified gauge, in our case the minimal Landau gauge

$$\sum_{x,\mu} \cos(\theta_{x,\mu}^G) \rightarrow \max \quad (2)$$

with respect to gauge transformations G , the propagator is written in terms of the Fourier transformed gauge potential,

$$\tilde{A}_{\vec{k},\mu} = \frac{1}{\sqrt{L^3}} \sum_{\vec{n}} \exp\left(2\pi i \sum_{\nu=1}^3 \frac{k_\nu (n_\nu + \frac{1}{2}\delta_{\nu\mu})}{L_\nu}\right) A_{\vec{n}+\frac{1}{2}\vec{\mu},\mu}, \quad (3)$$

which is a sum over a set of points $\vec{x} = \vec{n} + \frac{1}{2}\vec{\mu}$, the midpoints of the links in μ direction, which form the support of $A_{\vec{x},\mu}$ on the lattice. \vec{n} denotes the lattice sites (nodes) with integer Cartesian coordinates. The propagator is the gauge-fixed ensemble average of the following bilinear in \tilde{A} ,

$$D_{\mu\nu}(\vec{p}) = \langle \tilde{A}_{\vec{k},\mu} \tilde{A}_{-\vec{k},\nu} \rangle, \quad (4)$$

where the lattice momenta \vec{p} on the left hand side of (4) are related to the integer valued Fourier momenta \vec{k} by the expression (a is the lattice spacing):

$$p_\mu(k_\mu) = \frac{2}{a} \sin \frac{\pi k_\mu}{L_\mu}, \quad k_\mu = 0, \pm 1, \dots, \pm \frac{L_\mu}{2}. \quad (5)$$

The lattice equivalent of $p^2 = \vec{p}^2$ is in 3 dimensions

$$p^2(\vec{k}) = \frac{4}{a^2} \sum_{\mu=1}^3 \left(\sin \frac{\pi k_\mu}{L_\mu} \right)^2. \quad (6)$$

For this paper, we decided to identify the gauge field $A_{\vec{x},\mu}$ in terms of the sine function of the link angle (with $g_3^2 = 1/(a\beta)$)

$$A_{\vec{n}+\frac{1}{2}\vec{\mu},\mu} = \frac{1}{g_3 a} \sin \theta_{\vec{n},\mu}. \quad (7)$$

The corresponding propagator, called $D_{\mu\nu}^{\text{sin}}$ in Ref. [12], will be called simply $D_{\mu\nu}$ for brevity. The extraction of the Fourier transformed gauge field (and of its regular and singular components) has to be performed after the original gauge field configuration has been put into the minimal Landau gauge. The procedures employed for gauge fixing in the present context have been described at length in Ref. [12].

At zero temperature, for perfect Euclidean rotational invariance, the continuum propagator would be expressible by functions of p^2 . The most general tensor structure is then the following one including two scalar functions of p^2 ,

$$D_{\mu\nu}(\vec{p}) = P_{\mu\nu}(\vec{p}) D(p^2) + \frac{p_\mu p_\nu}{p^2} \frac{F(p^2)}{p^2} \quad (8)$$

with the three-dimensional transverse projection operator

$$P_{\mu\nu}(\vec{p}) = \delta_{\mu\nu} - \frac{p_\mu p_\nu}{p^2}. \quad (9)$$

The two structure functions $D(p^2)$ and $F(p^2)$ can be extracted by projection, on the lattice from $D_{\mu\nu}(\vec{p})$ according to (4), as

$$F(p^2) = \sum_{\mu,\nu=1}^3 p_\mu D_{\mu\nu}(\vec{p}) p_\nu \quad (10)$$

and

$$p^2 D(p^2) = \frac{1}{2} \sum_{\mu,\nu=1}^3 P_{\mu\nu}(\vec{p}) D_{\mu\nu}(\vec{p}). \quad (11)$$

They are approximately rotationally invariant, *i.e.* individual momenta \vec{p} might slightly differ in the function values D or F they provide, even if they have the same p^2 . Dense, in p^2 nearby data points may scatter rather than be forming a smooth function of p^2 .

In practice, using these definitions, we extract at first the function $F(p^2)$ from Eq. (10). In the sum the imaginary parts of non-diagonal $D_{\mu\nu}$ cancel. Then, $D(p^2)$ is obtained through

$$D(p^2) = \frac{1}{2} \left\{ \left[D_{11}(\vec{p}) + D_{22}(\vec{p}) + D_{33}(\vec{p}) \right] - \frac{F(p^2)}{p^2} \right\}. \quad (12)$$

For exactly fulfilled Landau gauge $F(p^2) \equiv 0$. On the lattice, in the case of the sine-definition used for $A_{\vec{x},\mu}$ [Eq. (7)], this is actually the case as soon as one of the local maxima of (2) (Gribov copies) is reached, with an accuracy which directly reflects the precision at stopping of the gauge fixing iterations.

The effect of monopoles (singular fields) can be distinguished from that of the regular (“photon”) fields using the splitting of the gauge field angles $\theta_{x,\mu}$ into a regular and a monopole part following Refs. [20, 11, 12]. In the notation of lattice differential forms this can be written as:

$$\theta = \theta^{\text{reg}} + \theta^{\text{mon}}, \quad \theta^{\text{mon}} = 2\pi\Delta^{-1}\delta p[j], \quad (13)$$

where Δ^{-1} is the inverse lattice Laplacian and the 0-form $*j \in \mathbb{Z}$ is nonvanishing on the sites of the dual lattice occupied by monopoles and antimonopoles. The 1-form $*p[j]$ corresponds to Dirac strings (living on the links of the dual lattice) which connect monopoles with antimonopoles, $\delta *p[j] = *j$. For any Monte Carlo configuration, we have fixed the gauge, then located the Dirac strings, $p[j] \neq 0$, and constructed the monopole part θ^{mon} of the gauge field according to the last equation in (13). The regular photon field² is taken just as the complement to the monopole part according to the first equation of (13).

The regular and the singular parts of the gauge field contribute to the propagator as follows: the total propagator decomposes like $D = D^{\text{reg}} + D^{\text{mon}} + D^{\text{mix}}$, where D^{mix} represents the mixed contribution from regular *and* singular fields. An analogous decomposition is valid for the longitudinal structure function F which vanishes to a good accuracy for the *total* propagator. In this paper we are interested mainly in the regular part and in the total photon propagator. To describe the propagators quantitatively we have fitted the total propagator using the following function:

$$D(p^2) = \frac{Z m^{2\alpha}}{\beta (p^{2(1+\alpha)} + m^{2(1+\alpha)})} + C, \quad (14)$$

where Z , α , m and C are the fitting parameters. This fit has been successfully used to describe the propagators of the finite and zero-temperature compact U(1) gauge model [11, 12] in 2 + 1 or 3 dimensions, respectively. The form is similar to some of Refs. [15] where the propagator in gluodynamics has been studied. The meaning of the fitting parameters in Eq. (14) is as follows: Z is the renormalization of the photon wavefunction, α is the anomalous dimension, m is a mass parameter. As shown in Ref. [12], in cQED₃ this mass parameter coincides with the Polyakov prediction [4] for the Debye mass, generated by the monopole-antimonopole plasma. The parameter C corresponds to a δ -like interaction in the coordinate space and, consequently, is irrelevant for long-range physics.

The regular (or “photon”) part of the propagator, D^{reg} , has been fitted by the Yukawa form (with an additional contact term):

$$D^{\text{reg}}(p^2) = \frac{Z_{\text{reg}}}{\beta (p^2 + m_{\text{reg}}^2)} + C_{\text{reg}}. \quad (15)$$

The fits together with the appropriate propagator data will be presented in the next section.

3 Numerical Results

We begin with the typical shape of the total photon propagator and its regular part, respectively, at fixed $\beta = 2.0$. The total photon propagator D , multiplied by p^2 , is shown in Figure 1(a) for various values of κ as a function of $|\vec{p}|$. We also present the fits of the data by the function (14). One clearly observes that the total propagator is well described by the fitting function in each particular case. The “infrared” enhancement at intermediate momenta disappears with

²In principle, the regular part of the links could have been reconstructed as well, without recurrence to the singular part. In this case the regular propagator would become *completely* independent of the number of Gribov copies N_G (see the discussion below).

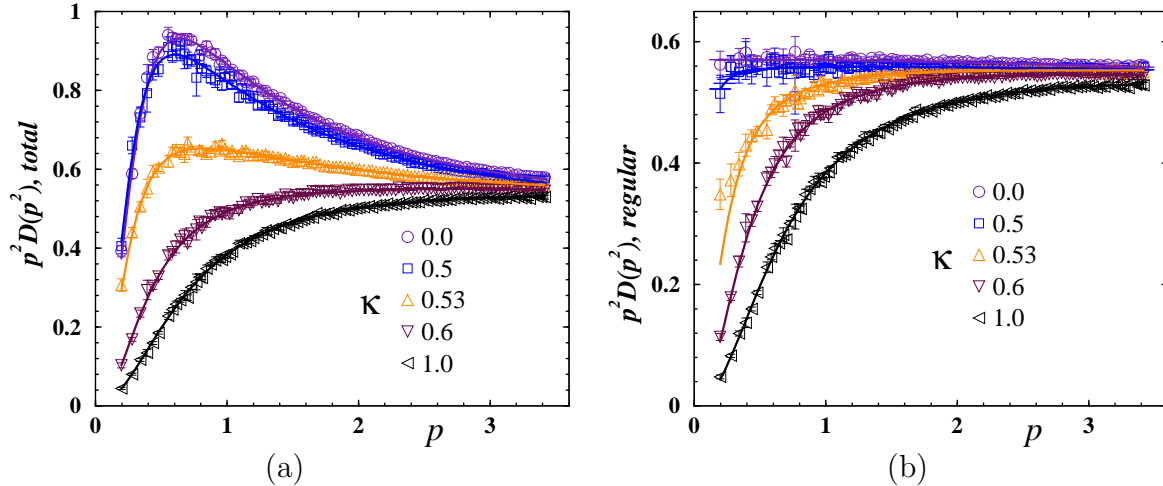


Figure 1: Momentum dependence of the total propagator (a) and its regular part (b) and fitted curves

increasing κ . In contrast, the suppression at very small $|\vec{p}|$ remains at all κ values. We can conclude that the total photon propagator is less singular in the infrared than a free one. According to our fitting function (14) the propagator is finite at $p^2 = 0$.

For comparison, the regular photon propagator part D^{reg} , multiplied by p^2 , is shown in Figure 1(b) for various values of κ . One can see that the behaviour of $D^{\text{reg}} \propto 1/p^2$ is only observed in the confinement region; in the Higgs region the propagator becomes massive. The fits using function (15) work very well everywhere except for smallest non-zero momenta in the closest vicinity of the crossover point.

Note that the data for both the total propagator and the regular part have been averaged over lattice momenta corresponding to the same p^2 before fitting (as in Refs. [11, 12]).

From the fits we have obtained the characterizing fit parameters for the transverse photon propagator D in gauge fixed ensembles with various numbers ($N_G \leq 100$) of Gribov copies. This means that, after applying the gauge fixing algorithm to N_G random gauge copies of the original Monte Carlo gauge field, only the configuration with the maximal value of the gauge fixing functional (2) is kept for evaluation. In Fig. 2 we show the dependence of the fit parameters for the total photon propagator on the number of Gribov gauge copies. Three typical κ values are used: $\kappa = 0.3$ in the confinement region, $\kappa = 0.535$ very near the crossover and $\kappa = 0.7$ in the Higgs region. While a moderate number $N_G \approx 30$ seems to be sufficient for convergence of all parameters at all κ values, there is no clear tendency between different κ 's. The parameters describing the regular propagator D^{reg} converge within the first few ($N_G \approx 5$) copies.

To keep the influence of N_G on the propagator negligible we have used in the final measurements $N_G = 60$. The resulting fit parameters of interest are presented in Fig. 3 as functions of κ . Fig. 3(a) depicts the mass taken from the fit (15) for the regular part of the propagator ("regular mass" m_{reg}), and from the fit (14) for the total propagator ("total mass", m). The dashed line represents the expected behaviour of the mass in the limit of large κ and β

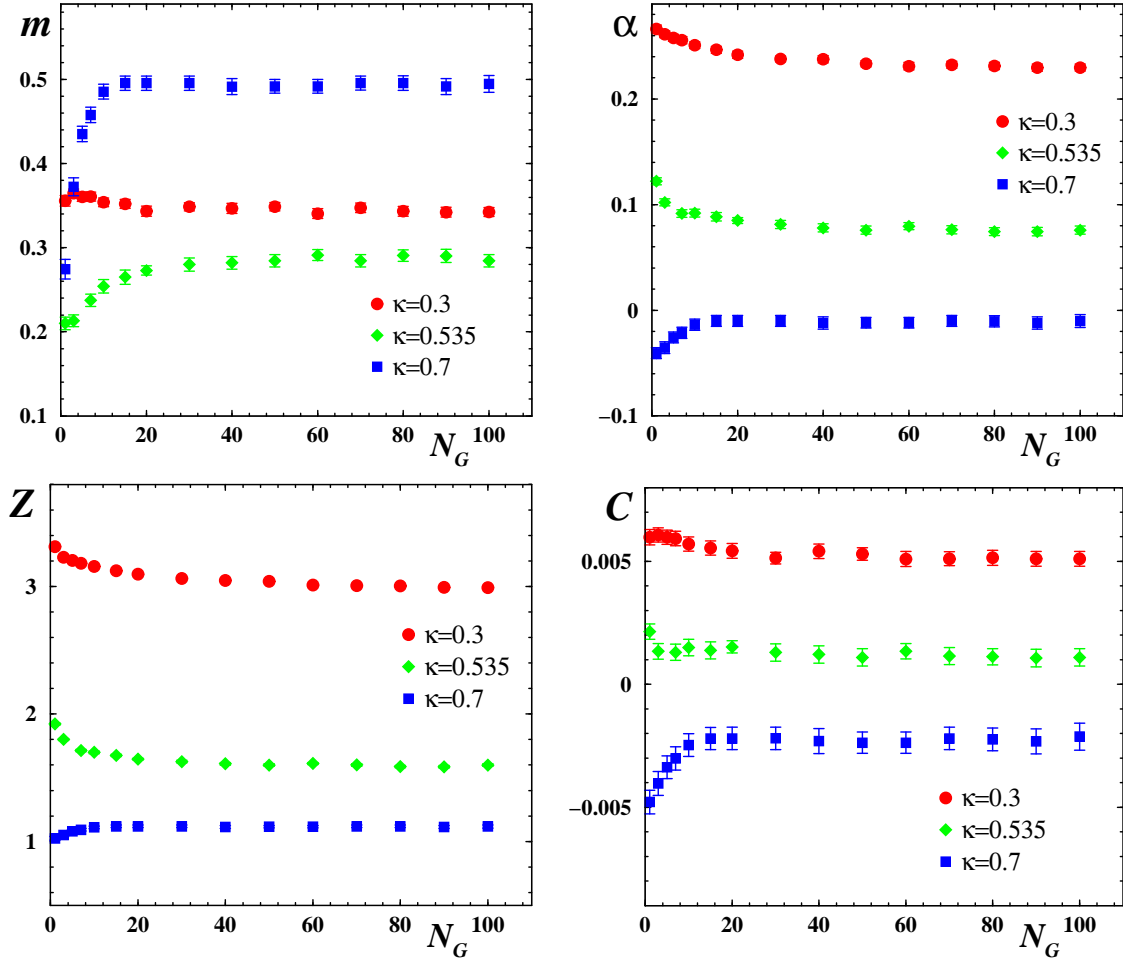


Figure 2: Dependence of the fit parameters m , α , Z and C on the number N_G of Gribov copies.

couplings:

$$m_{\text{th}}(\beta, \kappa) = \sqrt{\frac{\kappa_V(\kappa)}{\beta_V(\beta)}}, \quad (16)$$

where β_V and κ_V are the Villain couplings corresponding to the Wilson couplings β and κ . This parameterization is analogous to Ref. [21], with

$$\beta_V(\beta) = \left[2 \log \frac{I_0(\beta)}{I_1(\beta)} \right]^{-1}, \quad \kappa_V(\kappa) = \left[2 \log \frac{I_0(\kappa)}{I_1(\kappa)} \right]^{-1}. \quad (17)$$

Note, that although $\beta = 2.0$ (used in our calculations) is not very large, the first relation in Eq. (17) works with an accuracy of a few percent already at $\beta \sim 1$ according to the calculation [21] of the critical coupling in $4D$ cQED.

We observe that both the total and regular masses coincide with each other on the Higgs side of the crossover, and there they are very close to the prediction (16,17), the immediate

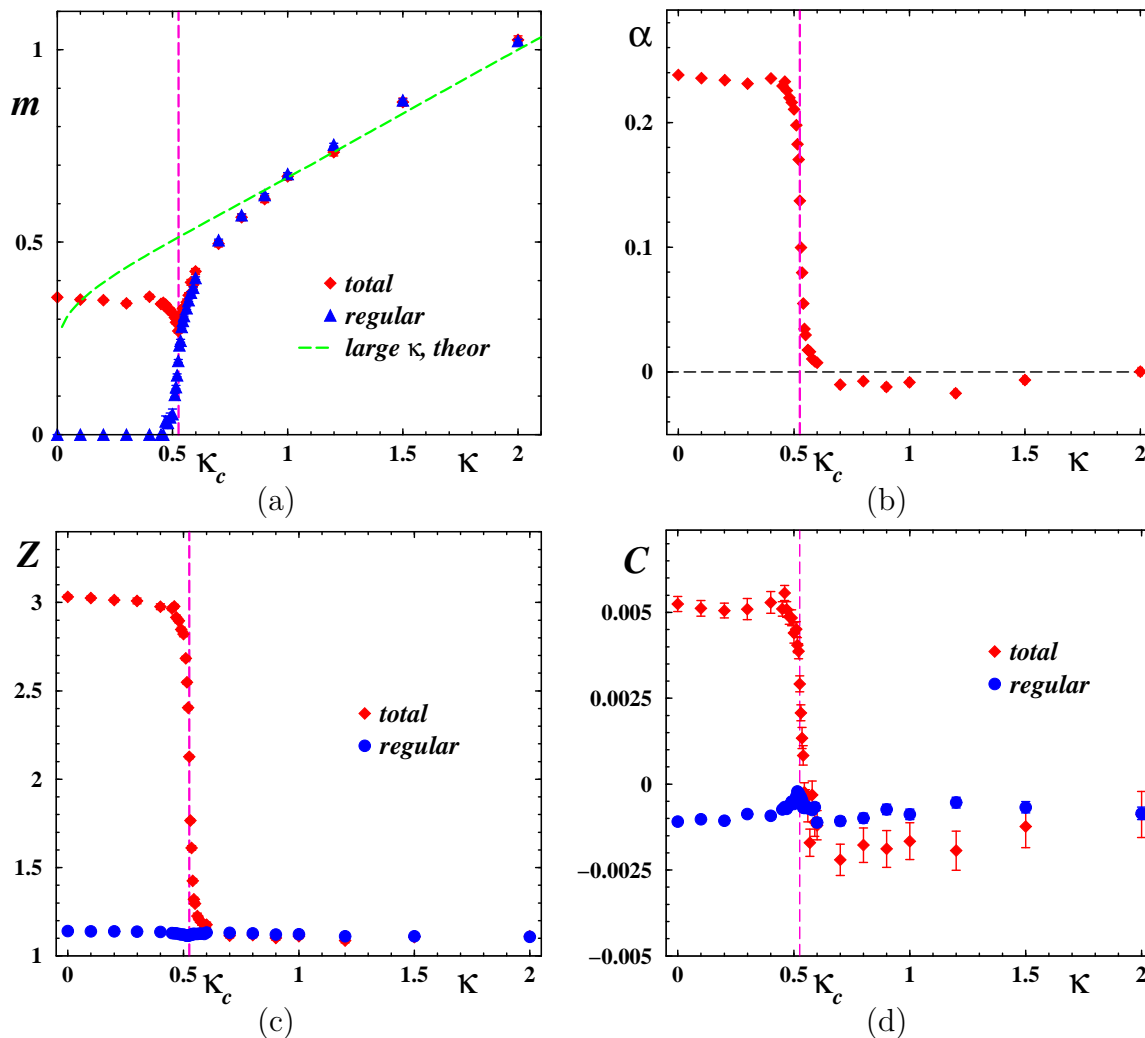


Figure 3: Fit parameters for the propagators at $\beta = 2.0$ as function of κ : (a) m and m_{reg} together with the analytical prediction for large κ ; (b) α ; (c) Z and Z_{reg} and (d) C . The crossover point is denoted by the vertical dotted line.

vicinity of the crossover point excluded. This observation can be easily understood. Two different sources contribute to the gauge boson mass: one is arising nonperturbatively from the monopoles (the Debye screening mass) while the other is due to the explicit presence of the mass term in the action (1) of the model. The Debye mass generation works in the case of the monopole–antimonopole plasma [4] and it is obviously absent in the magnetic dipole gas [6]. Since at large κ monopoles and antimonopoles are bound into dipoles [3, 5], the Debye contribution to the mass disappears, and the gauge boson mass is exclusively given by Eq. (16). As can be seen from Fig. 3(a), at small κ values the total mass m is close to the Debye mass of pure cQED₃ (*i.e.* to the mass value at $\kappa = 0$) because the effects of the mass term in the action (1) are small. Moreover, in accordance with our expectations, the regular mass m_{reg} vanishes.

In the region very close to the crossover, $\kappa \approx \kappa_c$, the mass m shows a minimum caused, as one could guess, by the interference between perturbative mass and Debye mass effects. Indeed, as κ tends to κ_c , the Debye mass gets smaller since the density of the monopole–antimonopole plasma drops rapidly. On the other hand, the perturbative mass term becomes more significant. The interplay of these two tendencies results in the noticed minimum at $\kappa \approx \kappa_c$.

In Fig. 3(b) we show the anomalous dimension α for the total propagator³ as a function of the hopping parameter κ . The anomalous dimension is non-vanishing in the confined region and it turns to trivial values at the crossover⁴, $\alpha \rightarrow 0$. This behaviour can be compared with our studies of compact QED₂₊₁ at finite temperature [11, 12]: in the monopole–antimonopole plasma phase (corresponding to the confinement side) $\alpha > 0$ while in the magnetic dipole phase (corresponding to the Higgs side) $\alpha = 0$. Thus, in cAHM the effect of the monopole pairing on the propagator is the same as in cQED: the anomalous dimension gets close to zero in the Higgs phase dominated by the magnetic dipole gas.

Similarly to the anomalous dimension, the effect of the monopole pairing on the renormalization parameter Z of the photon wavefunction in cAHM, shown in Figure 3(c), is remarkably similar to the cQED case observed⁵ in Refs. [11, 12]. The total photon factor Z suddenly drops at the crossover point, $\kappa = \kappa_c$ while the regular factor, Z_{reg} , is almost insensitive with respect to the crossover ($Z \rightarrow Z_{\text{reg}} \approx 1$ for all κ values). The small contact term parameter of the total propagator, C , changes its sign at the crossover, Figure 3(d). The small and negative contribution of C_{reg} in the confinement is responsible for the tiny decrease of the massless $p^2 D^{\text{reg}}$ with p^2 [seen at zero and small κ in Fig. 1(b)]. A zoom to the crossover region is shown in Fig. 4,

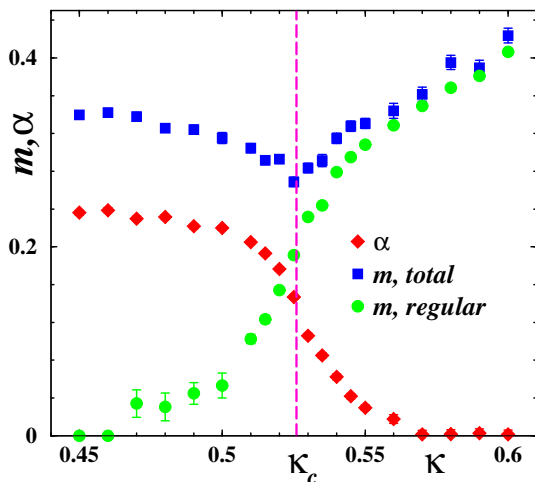


Figure 4: Zoom to masses and anomalous dimension in the crossover region.

³Recall, that the anomalous dimension for the regular part of the propagator is zero, Eq. (15).

⁴The 4-parameter fits lead even to small negative α in the region $\kappa \sim 1$. However, fitting there the propagators with *fixed* $\alpha = 0$, the obtained masses coincide within errors with those of the unconstrained fits. So we associate this behaviour with statistical fluctuations.

⁵ Due to an error, the Z factors in Figs. 5c and 7c of Ref. [12] need to be corrected by a factor m^α before they can be compared with the Z given here at $\kappa = 0$.

where all effects described above for m , m_{reg} and α are seen more clearly together.

4 Conclusions

In our numerical studies we found that the gauge boson propagator in the London limit of the three-dimensional compact Abelian Higgs model possesses a non-zero anomalous dimension below the string breaking crossover. The effects of the matter fields on the propagator are remarkably similar to the finite-temperature deconfining effects in the pure gauge compact $U(1)$ model. Both in the Higgs (deconfinement) region of cAHM and in the deconfinement (high temperature) phase of cQED the anomalous dimension of the propagator vanishes. In the confining regions of both models the anomalous dimension is non-vanishing. The positive anomalous dimension is due to presence of the monopole-antimonopole gas in the plasma state [11]. As we move towards the deconfinement phase α decreases and becomes zero when the monopole-antimonopole plasma turns into a magnetic dipole gas. However, the origin of the pairing phenomenon in both models is different: in cAHM the monopole pairing is caused by the matter fields [3] while in cQED the monopoles form the bound states due to temperature effects in the monopole-antimonopole interaction.

For the limit of cAHM with frozen radial Higgs degrees of freedom we have found that the anomalous dimension for the gauge field does not become clearly negative together with the onset of string breaking. However, if radial fluctuations of the Higgs field would be allowed, the emergence of a negative anomalous dimension cannot be ruled out [22, 3].

The mass in the gauge boson propagator closely follows the tree level expectations on the Higgs side of the transition and simply corresponds to a massive Yukawa propagator practically unaffected by remaining dipoles in the vacuum. In the confinement region the mass related to the total gauge field is of Debye type while the mass of the regular or photon part of the gauge field degrees of freedom remains massless.

Acknowledgements

M. N. Ch. is supported by the JSPS Grant No. P01023. E.-M. I. acknowledges useful discussions with L. von Smekal.

References

- [1] E. H. Fradkin and S. H. Shenker, Phys. Rev. **D 19** (1979) 3682.
- [2] M. B. Einhorn and R. Savit, Phys. Rev. **D 17** (1978) 2583; *ibid.* **D 19** (1979) 1198.
- [3] H. Kleinert, F. S. Nogueira and A. Sudbø, Phys. Rev. Lett. **88** (2002) 232001; hep-th/0209132.
- [4] A. M. Polyakov, Nucl. Phys. **B 120** (1977) 429.
- [5] M. N. Chernodub, E.-M. Ilgenfritz and A. Schiller, Phys. Lett. **B 547** (2002) 269.

- [6] M. N. Chernodub, Phys. Rev. **D 63** (2001) 025003; Phys. Lett. **B 515** (2001) 400.
- [7] V. L. Berezinsky, Sov. Phys. JETP **32** (1971) 493,
J. M. Kosterlitz, D. Thouless, J. Phys. **C 6** (1973) 1181.
- [8] N. O. Agasian and D. Antonov, Phys. Lett. **B 530** (2002) 153.
- [9] N. Parga, Phys. Lett. **B 107** (1981) 442;
N. O. Agasian and K. Zarembo, Phys. Rev. **D 57** (1998) 2475.
- [10] M. N. Chernodub, E.-M. Ilgenfritz and A. Schiller, Phys. Rev. **D 64** (2001) 054507; *ibid.* **D 64** (2001) 114502.
- [11] M. N. Chernodub, E.-M. Ilgenfritz and A. Schiller, Phys. Rev. Lett. **88** (2002) 231601.
- [12] M. N. Chernodub, E.-M. Ilgenfritz and A. Schiller, hep-lat/0208013, Phys. Rev. **D**, in press.
- [13] V. N. Gribov, Nucl. Phys. **B 139** (1978) 1.
- [14] C. Alexandrou, P. de Forcrand and E. Follana, Phys. Rev. **D 63** (2001) 094504; *ibid.* **D 65** (2002) 114508.
- [15] P. Marenzoni, G. Martinelli and N. Stella, Nucl. Phys. **B 455** (1995) 339;
D. B. Leinweber, J. I. Skullerud, A. G. Williams and C. Parrinello, Phys. Rev. **D 60** (1999) 094507;
A. G. Williams, in *Proc. of 3rd Int. Conf. on Quark Confinement and Hadron Spectrum*, hep-ph/9809201;
J. P. Ma, Mod. Phys. Lett. **A 15** (2000) 229.
- [16] K. Langfeld, H. Reinhardt and J. Gattnar, Nucl. Phys. **B 621** (2002) 131.
- [17] A. Cucchieri and D. Zwanziger, Phys. Lett. **B 524** (2002) 123.
- [18] D. Zwanziger, Nucl. Phys. **B 364** (1991) 127.
- [19] A. Nakamura and M. Plewnia, Phys. Lett. **B 255** (1991) 274;
M. I. Polikarpov, K. Yee and M. A. Zubkov, Phys. Rev. **D 48** (1993) 3377;
V. G. Bornyakov, V. K. Mitrjushkin, M. Müller-Preussker and F. Pahl, Phys. Lett. **B 317** (1993) 596;
I. L. Bogolubsky, V. K. Mitrjushkin, M. Müller-Preussker and P. Peter, Phys. Lett. **B 458** (1999) 102.
- [20] R. Wensley and J. Stack, Phys. Rev. Lett. **63** (1989) 1764;
H. Shiba and T. Suzuki, Phys. Lett. **B 333** (1994) 461.
- [21] T. Banks, R. Myerson and J. B. Kogut, Nucl. Phys. **B 129** (1977) 493.
- [22] I. F. Herbut and Z. Tesanovic, Phys. Rev. Lett. **76** (1996) 4588.